

A vast-range speed control microchip for retention of all cell types†

Xing Yue (Larry) Peng,^{*a} Ling Qiao Li^a and Hua Sheng Hong^b

Received 22nd October 2008, Accepted 29th June 2009

First published as an Advance Article on the web 8th July 2009

DOI: 10.1039/b818738j

This Technical Note is the first description of a large-scale logarithmic flow-rate damping system designed to retain cells of different adherence, different suspensibility and different motility. The chamber, which can easily retain and cultivate many types of cells, including high-motility cells and swimming cells, *via* a series of “speed bumps”, readily facilitates cell retention for complex heterogeneous cultures. Yeast cells, red blood cells, rabbit bone marrow aspirate and dinoflagellate swimming cells were introduced into the chip for multi-cell retention, multi-cell culture and observation. Here, we show that the chamber creates a flow field with a ratio of end/start speeds as low as 0.01. The logarithmic distribution of flow-rate within the chamber is controlled precisely by pressure, all of the cell types that we tested were retained easily within the chamber. Many cell–cell interactions were observed, predicting a high potential for the success of on-chip heterogeneous cell experiments.

Introduction

The construction of a heterogeneous cell-based microenvironment¹ for single cells in a microfluidic device is a huge challenge,² which must be met successfully for the development of biologically routine application of ‘cells on chips’. The ability to manipulate and retain cells is achieved by making use of hydrodynamic, gravitational, or adhesion forces.³ The basic shape of most microfluidic chambers is rectangular,^{2–6} but they are limited by their narrow range of flow velocity for retention of different cell types with a wide range of adhesion ability, suspensibility and motility for on-chip co-culture. Multi-cell micropatterning² makes use of the strong adhesion force of cells or gel modules.⁴ For weak adhesion, the chamber can be put into a side channel,^{7,8} filled with sieves^{9,10} or microfibers,¹¹ or the shape can be changed to circular^{8,9,12} with terraces¹² to expand the velocity distributions for more cell types. The Hele-Shaw¹³ flow chamber is an expanding diameter chamber that has proved useful for cell capture, but it is not a broadband flow-rate chamber. Its high/low or inlet flow rate/outlet flow rate ratio is only ~ 3 . The objective of this work was to design a chip that can retain a wide variety of cell types, including suspending cells (like red blood cells), low-motility cells (like leukocytes), and high-motility (swimming) cells (like sperm or dinoflagellates), and to aim for co-cultures.

We designed a trumpet-like chamber with a logarithmic expansion to create a great range of flow-rates for a wide variety of cell types. The original flow-rate in the trumpet-like chamber can be slowed to less than 1/100. Even when the inlet flow is very fast, the outlet flow can be very slow and will provide very low shear stress. For very high-motility cells, such as swimming cells,

the high flow-rate at the inlet can guarantee cell injection and prevent cells from escaping the inlet by swimming backward, and the very slow flow-rate near the outlet provides low shear stress for the cell culture. Speed bumps are embedded in the open area to aid the function of the speed-control chamber.

Experimental

The predictability and controllability determine the quality of the chamber. Logarithmic or exponential functions are natural functions of variables such as loudness, brightness or even the size of cells; exponential widths, not linear widths, are logarithmically even and the whole chamber is effective for better predictability and controllability. The streamlines in a speed-control chamber follow an approximate exponential curve, (Fig. 1A,B) which has a calculable length (see ESI†), and are straight only along the central axis. Speed bumps are designed to follow a path of the same length as these curves. The precision of the pressure control is ± 0.5 Pa for pressure (Anthone Elec. Ltd., Xiamen, China). The etching depth is strictly controlled to form speed bumps according to Fig. 1C. Higher h_2 facilitates cell adhesion, while a very low h_1 can block the flow with cells. We tried to label the micro-flows in the chamber with chicken red blood cells. Velocities of moving cells were calculated for statistical evaluation of the velocity of the liquid flow. Rabbit bone marrow cells were collected from the bones of domesticated rabbits. *Alexandrium tamarense* cells were cultured for the injection of swimming cells (see ESI for details†).

Results and discussion

Microfluidic tests

The resistance of viscous liquid flow in a tube is related directly to its velocity. Therefore, a linear relationship is expected between pressure and velocity in the speed-control chamber. Fig. 2A shows the correlation of velocity and pressure in a large data set. Apart from the slight bending of the fitted curve caused by friction between the red blood cells and the floor of the chip at

^aDepartment of Biology, Xiamen University, Xiamen, Fujian, 361005, China. E-mail: xypeng@xmu.edu.cn; Fax: +86-592-2181386; Tel: +86-592-2181386

^bState Key Laboratory for Marine Environmental Science, Xiamen University, Xiamen, 361005, China

† Electronic supplementary information (ESI) available: Detail experimental and results in text with figures and six movies. See DOI: 10.1039/b818738j

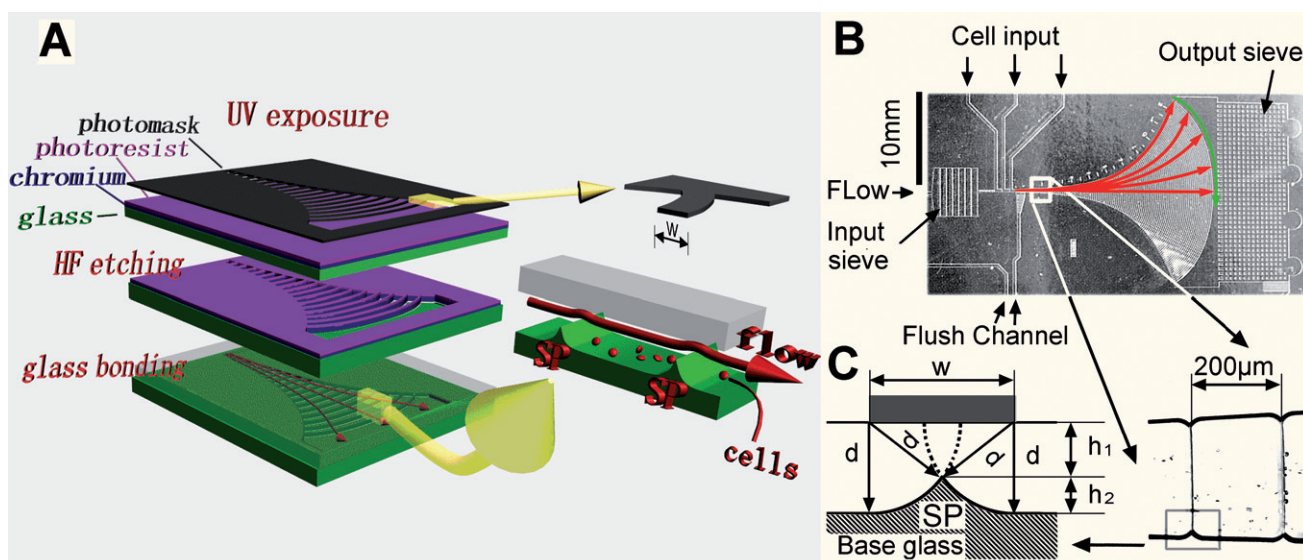


Fig. 1 The manufacture of a speed-control chip with speed bumps. **A** One-step photomask exposure, etching and bonding for both the trumpet-like chamber and its speed bumps (SP). **B** A real glass chip with a speed-control chamber. Red arrows show the streamlines, and the green arrow shows a curve that has the same distance along the streamlines from the entrance. Speed bumps are designed according to different lengths of streamlines from the entrance. **C** Dimensions of speed bumps (h_1 and h_2) are controlled by the mask width (w) and the etching depth (d).

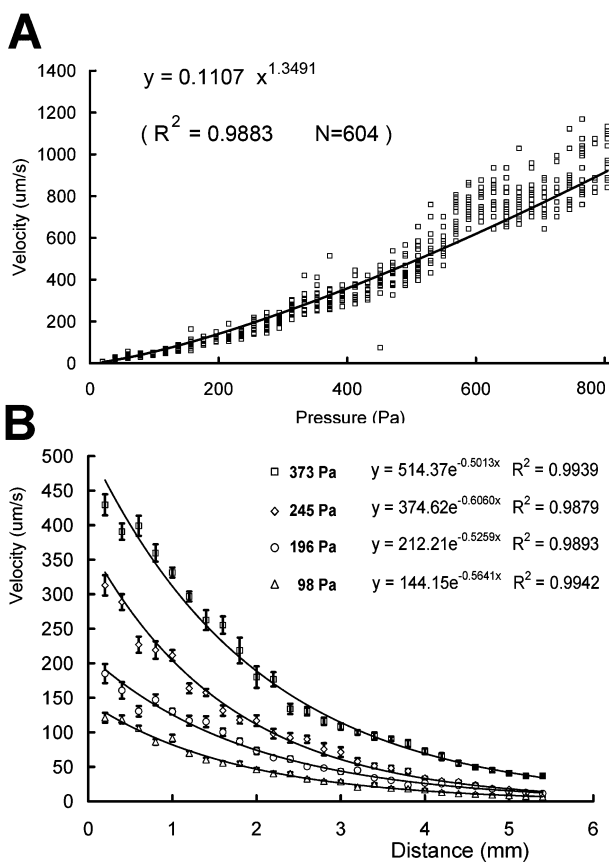


Fig. 2 The pressure control on the entrance velocity (**A**) and the velocity distributions (**B**) in a speed-control chamber. Each point represents a single measurement of a red blood cell by analyzing the video. Error bars represent average standard deviations from at least 12 replicates.

a low flow rate, the velocity–pressure model gives the speed-control chamber a practical application under precise speed control. An ideal speed-control chamber requires a logarithmic distribution of flow-rate. Velocities of cells are used to substitute velocities of flow. Thousands of moving red blood cells were measured by analyzing video clips, and the results are illustrated by Fig. 2B. The results are logical and smooth, and curve fitting of a logarithmic model revealed very similar coefficients (-0.50 at 373 Pa, -0.60 at 245 Pa, -0.53 at 196 Pa, and -0.56 at 98 Pa). By combining the pressure–velocity model and the distance–velocity model, velocities from 1000 $\mu\text{m/s}$ to 0 were controlled precisely by the speed-control chamber. The ratio of end/start speeds can be as low as 0.01.

To evaluate the chamber's ability to retain specified types of cells, we used yeast cells to measure the distributions in the process of pressure-driven sample movements along the speed-control chamber; the results are shown in Fig. 3A. The high cell density sample sections formed peaks in the cell distribution diagrams. There was a high and narrow peak near the chamber entrance (see the left-hand peak), and the peak expanded as it moved toward the outlet (from left to right). While the peak expands, cells in the sample are dispersed and physical details are magnified. Any tiny differences among cells emerge on the peaks. From the four distributions in Fig. 3A, two sub-groups are separated (see the peaks on the right, labeled with the highest pressure). Here, the cell-affinity chromatographic effect is apparently based on a cell's suspensibility or adherence. Further inspections under the microscope showed that the faster group had more cell clusters (see images in ESI†). Our previous studies of on-chip growth of yeast cells¹⁴ showed that multi-cell clusters were formed by the consecutive budding of cells; *i.e.* the cell clusters are younger cells.

Rabbit bone marrow cells were used to test the additional retaining effects of speed bumps (Fig. 3B). The distribution

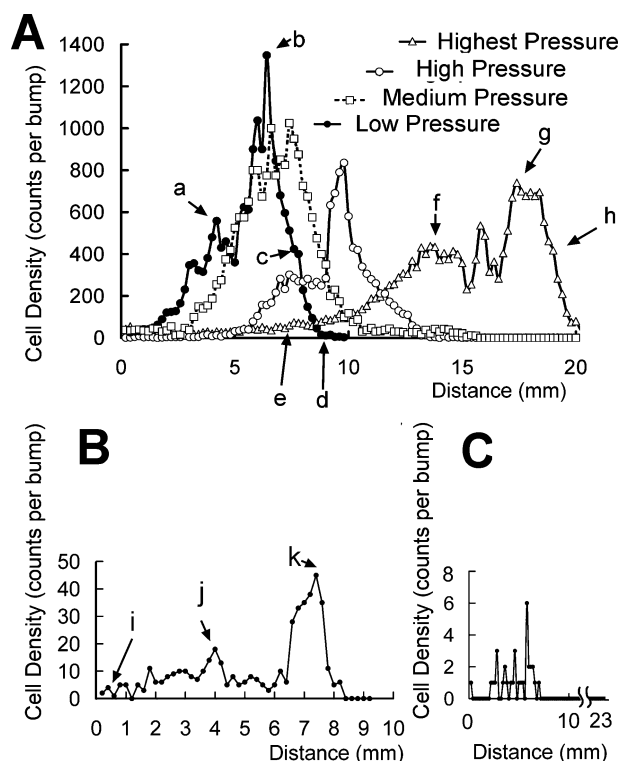


Fig. 3 The density distributions of different cells (**A**, yeast cells; **B**, rabbit bone marrow cells; **C**, fast swimming dinoflagellate cells. The images at a–k and other details can be found in ESI†)

shows an abrupt stopping head caused by the blocking effect when the velocity is sufficiently low, and a long tail caused by the difference between cells and larger cells that were blocked earlier. The stopping distance is controlled by the pressure of the sample injection; the lower the sample injection pressure, the shorter the stopping distance. Fig. 3C shows the results for swimming cells. The stopping distance is also controlled at ~ 8 mm.

Multi-cell cultures of rabbit bone marrow aspirate

Cells from bone marrow aspirate show a high level of vitality in the chamber. Some of them can spin with the flow. Leukocytes

move across speed bumps at a speed of about $10 \mu\text{m}/\text{min}$ (see ESI†). The chemotactic migration of leukocytes during incubation for ~ 19 h is shown in Fig. 4A. The flow-rate was $8 \mu\text{m}/\text{s}$. The two cells (L2 and S1) were spatially very close (within $10 \mu\text{m}$) at first but showed no relationship at the beginning. After 3 h and 28 min, L2 developed from a round and smooth bone marrow cell into an amoeba-like leukocyte. L2 then passed downstream and, ignoring the existence of S1. After 4 h, L2 had a chemotactic response (see the 8-shaped yellow line), went upstream and up the slope (energy-consuming moving) to catch S1 and turned downstream without hesitation. L2 maintained strong contact with S1 in the next 14 h but did not invaginate or destroy S1. Once or twice S1 nearly escaped from L2 and was retained (See ESI movie†).

Leukocytes carrying small cells were common in the video clips. A leukocyte (L3) carrying a small cell (S2) is traced in a series of images in Fig. 4B. This L3 delivered its captive (S2) to a bone marrow cell (M2), but the captive was taken by another leukocyte (L4). The series of images in Fig. 4B follows this process for 34 min (see ESI movie†). Leukocyte L3 went upstream and carried a small cell (S2). Its velocity was about $5 \mu\text{m}/\text{min}$ toward a bone marrow cell (M2), and 4 min later L3 was very close to M2. There was an obvious contact between L3 and M2 for 2 min, and if there was any exchange of molecular information between L3 and M2, it must have occurred during this time. We know that a leukocyte carrying a cell holds its captive very tightly, and controls it for >14 h. But at this time, L3 drops S2, moves far away and does not return. In the meantime, another hunter leukocyte, L4, emerges from downstream and steals S2, turns downstream, crosses the peak of the speed bump and moves far away (see Fig. 4B and ESI†).

The paradoxical roles of the immune system during cancer development^{15,16} are a good reason to question methods that lack the means to observe single cells directly in the context of a diverse range of cell types. As the most dangerous cancer cell metastasis is definitely a kind of physical transportation. We suggest that this direct carrying and delivering act of leukocytes may be a metastatic method of cancer cells. Macrophages are prominent in the stromal compartment in virtually all types of malignancy.^{17,18} Apparently, macrophage recruitment and poor prognosis indicate that macrophages are crucial for facilitating late-stage metastatic progression of tumors.¹⁵ However, apart

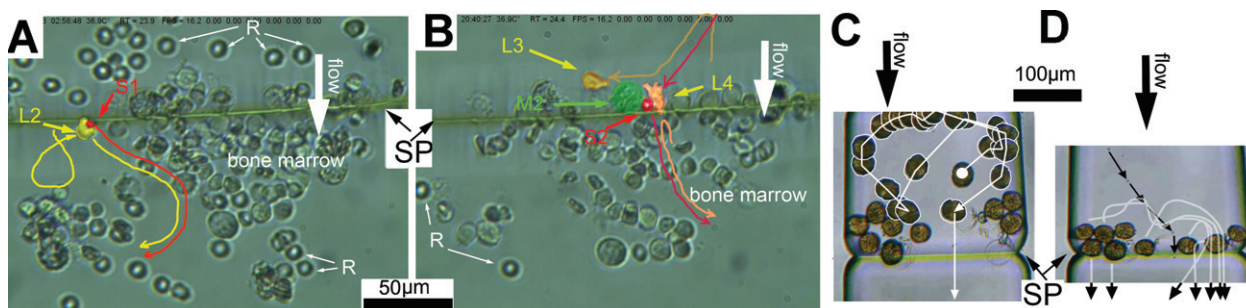


Fig. 4 On-chip cultures of rabbit bone marrow cells (**A**, **B**) and fast swimming dinoflagellate cells (**C**, **D**). Cells discussed in the text are coloured yellow or orange (leukocyte, L2, L3 and L4), green (spinning bone marrow cell, M2) and red (captive cells, S1 and S2). Lines of the same colour in **A** and **B** trace chemotactic movements or cell catching-carrying actions. The white lines in **C** indicate the path taken by one swimming cell with a series of overlapping images taken at 1 second intervals, and cells held in front of a speed bump. Each black arrow in **D** depicts the flow of a particle with images taken at 1 second intervals, and the white lines depict the pathway of seven cells germinating and crossing the speed bump (see ESI†). SP, speed bump.

from hypoxia, little is known of micro-environmental signals that regulate the activities of subpopulations of TEMs in these different tumor sites.¹⁸ Relationships between immune cells and metastasis are studied more by chemical than physical means, and the possibility of direct transportation of cancer cells by immune cells has not been explored.

Looking back at the on-chip experiments on rabbit bone marrow cells, we find that cells in the microchip are like a simulated immune system stimulated possibly by anoxia. A glass microchip prevents gas exchange with the culture medium, and oxygen is carried by the liquid flow and anoxia occurs, to some extent, in the chip. This is similar to the anoxia in a tumor, where the cancer cells use increasing amounts of oxygen and the blood flow cannot meet the demands. Either surgical wounds or anoxia of a big tumor may enable immune cells to be metastatic helpers. On the basis of our on-chip observations, our assumption is that active immune cells obtain the ability to carry cells a long way and they can drop the captured cells when they contact a marrow cell. This carrying and dropping action might be a basic function of most macrophages. If the anoxia area of a tumor attracts more and more macrophages, the direct carrying of macrophages moving in and out of this dangerous area will eventually cause metastasis of the cancer. Additionally, if macrophages release their cargo to bone marrow cells, bone marrow can be the first transfer station in the cancer metastasis.

Many questions arise from these on-chip results. Does the carrying act have a destination? Do similar phenomena exist in the human body, or in other mammals? If the carrying and dropping acts are common in mammals, what is its evolutionary significance? Is it the main metastatic method of cancer cells? How can we develop molecules to prevent leukocytes from carrying and dropping cells with preference for marrow cells? As a leukocyte can carry its captive cell through the narrow gap over speed bumps, can a leukocyte carrying a cancer cell go through the narrow gaps among tissue cells for metastasis?

Swimming cell cultures of dinoflagellate

A sperm cell uses its flagellum to propel itself toward the female oocyte at a speed of 0–35 $\mu\text{m/s}$.¹⁹ Culturing high-motility single cells is a great challenge for microfluidic microchips. The single cell motile phytoplankton *Prorocentrum micans* has been reported to be controlled successfully via the oscillation amplitude.²⁰ We tested the chip for multi-cell retention of high-motility *A. tamarense* single cells (speed of $\sim 50 \mu\text{m/s}$) (Fig. 3C). Fig. 4C shows retained cells and a well-balanced flow ($\sim 50 \mu\text{m/s}$). This weak flow maintains the supply of nutrients to the on-chip cells. Suitable flows suppress cyst cells slightly on the speed bump slopes and effectively guard the entrance of the chamber from any reverse escape of fast swimming cells. Unarmored cells can squeeze over speed bumps to the next step by virtue of flow pressure until cells can no longer benefit from flow pressure to cross bumps. Fig. 4D shows cells germinating from cysts and going to the next step of the chamber (see ESI†).

Conclusions

A speed-control chamber is designed to cover a great range of flow-rates. With a high velocity entrance and a low velocity

ending (flow-rate $< 1/100$ that of the entrance flow), a speed-control chamber easily retains all types of cells by pressure control and the chamber's logarithmic flow-rate distribution. Speed bumps are embedded into the large open area of the chamber to help it to retain low-or high-motility cells. Whole rabbit bone marrow cells and red tide dinoflagellate single cells were used to test the speed-control chamber for the range of ability for cell retention and culture. The results show that this chamber design is capable of retention and culture of all types of cells, including high-motility cells such as leukocytes, or swimming cells such as dinoflagellates (moving like sperm). Many cell-cell phenomena are observed in the multi-cell chamber, suggesting a high potential for on-chip heterogeneous cell experiments.

Acknowledgements

This work was supported by Anthon Elec. Ltd. (Xiamen, China) and the National Natural Science Foundation of China. The microchip fabrication by the Key Laboratory for Chemical Biology of Fujian Province is much appreciated. We thank Prof. T. L. Zheng for providing *Alexandrium tamarense*, Prof. Y. L. Zhou and Prof. L. Ren for valuable suggestions, N. Zhang, Y. Chen and H. J. Li for microchip fabrication, G. Y. He for algae maintaining, L. H. Peng and L. Q. Wu for cell counting and Y. Sha and S. Y. Tian for their contribution to the art work. We specially thank Leah Pan for English revision.

References

- 1 M. J. Bissell and M. A. LaBarge, *Cancer Cell*, 2005, **7**, 17–23.
- 2 A. L. Paguirigan and D. J. Beebe, *BioEssays*, 2008, **30**, 811–821.
- 3 S. M. Kim, S. H. Lee and K. Y. Suh, *Lab Chip*, 2008, **8**, 1015–1023.
- 4 D. A. Bruzewicz, A. P. McGuigan and G. M. Whitesides, *Lab Chip*, 2008, **8**, 663–671.
- 5 X. Song, B. Kong and D. Li, *Biotechnol Lett.*, 2008, **30**, 1537–1543.
- 6 S. M. Ong, C. Zhang, Y. C. Toh, S. H. Kim, H. L. Foo, C. H. Tan, D. Noort, S. Park and H. Yu, *Biomaterials*, 2008, **29**, 3237–3244.
- 7 R. Gomez-Sjoberg, A. A. Leyrat, D. M. Pirone, C. S. Chen and S. R. Quake, *Anal. Chem.*, 2007, **79**, 8557–8563.
- 8 K. Liu, R. Pitchamani, D. Dang, K. Bayer, T. Harrington and D. Pappas, *Langmuir*, 2008, **24**, 5955–5960.
- 9 M. C. Kim, Z. Wang, R. H. W. Lam and T. Thorsen, *Journal Of Applied Physics*, 2008, **103**(1–6), 044701.
- 10 Z. Wang, M. Kim, M. Marquez and T. Thorsen, *Lab Chip*, 2007, **7**, 740–745.
- 11 C. M. Hwang, A. Khademhosseini, Y. Park, K. Sun and S. H. Lee, *Langmuir*, 2008, **24**, 6845–6851.
- 12 S. Sugiura, J. Edahiro, K. Kikuchi, K. Sumaru and T. Kanamori, *Biotechnology and Bioengineering*, 2008, **100**, 1156–1165.
- 13 A. Sin, S. K. Murthy, A. Revzin, R. G. Tompkins and M. Toner, *Biotechnology and Bioengineering*, 2005, **91**, 816–826.
- 14 X. Y. Peng and P. C. H. Li, *Anal. Chem.*, 2004, **76**, 5282–5292.
- 15 K. E. de Visser, A. Eichten and L. M. Coussens, *Nature Reviews Cancer*, 2006, **6**, 24–37.
- 16 M. J. Bissell and D. Radisky, *Nature Reviews Cancer*, 2001, **1**, 46–54.
- 17 M. den Ouden, J. M. H. Ubachs, J. E. G. M. Stoot and J. W. J. van Wersch, *European Journal of Obstetrics & Gynecology and Reproductive Biology*, 1997, **72**, 73–77.
- 18 C. E. Lewis and J. W. Pollard, *Cancer Res.*, 2006, **66**, 605–612.
- 19 M. Bergh, S. Emiliani, J. Biramane, A. S. Vannin and Y. Englert, *Human Reproduction*, 1998, **13**, 3103–3107.
- 20 B. R. Lutz, J. Chen and D. T. Schwartz, *Anal. Chem.*, 2006, **78**, 5429–5435.